Journal of Molecular Graphics and Modelling 28 (2010) 792–798

Contents lists available at ScienceDirect

Journal of Molecular Graphics and Modelling

journal homepage: www.elsevier.com/locate/JMGM

Identification of potent urease inhibitors *via* ligand- and structure-based virtual screening and *in vitro* assays

Khalid M. Khan [a,*], Abdul Wadood [b,1], Muhammad Ali [a,1], Zia-Ullah [a], Zaheer Ul-Haq [b,*], M. Arif Lodhi [a], Momin Khan [a], Shahnaz Perveen [c], M. Iqbal Choudhary [a]

[a] H.E.J. Research Institute of Chemistry, International Center for Chemical and Biological Sciences, University of Karachi, Karachi 75270, Pakistan
[b] Panjwani Center for Molecular Medicine and Drug Research, International Center for Chemical and Biological Sciences, University of Karachi, Karachi 75270, Pakistan
[c] PCSIR Laboratories Complex, Karachi, Shahrah-e-Dr. Salimuzzaman Siddiqui, Karachi 75280, Pakistan

ARTICLE INFO

Article history:
Received 27 August 2009
Received in revised form 5 February 2010
Accepted 9 February 2010
Available online 17 February 2010

Keywords:
Virtual screening
2-aminothiophene
Urease inhibition
Phytotoxicity

ABSTRACT

A pharmacophore model was developed based on three structurally diverse urease inhibitors by using the GASP program. This model comprises the positions and tolerance for two acceptor atoms (AA1 and AA2), one donor atom (DA1), and one hydrophobic center (HYP1). This derived phamacophore model was employed to screen an *in-house* database of organic compounds. Hits obtained were evaluated by molecular docking using GOLD software. On the basis of ligand- and structural-based predictions, an *in vitro* testing of short-listed compounds was conducted and a novel class of urease inhibitors (2-aminothiophines) was identified. The potent *in vitro* activity and selectivity of these compounds, along with their non-toxic nature against the plant cells indicated that they can serve as leads for solving urease-associated health and agriculture problems.

1. Introduction

The metalloenzyme urease (urea amidohydrolase; EC 3.5.1.5) catalyzes the hydrolysis of urea into ammonia and carbon dioxide. It is present in a variety of plants, algae, fungi and bacteria [1–4]. Urease is involved in the pathogenesis of hepatic encephalopathy, hepatic coma urolithiasis, pyelonephritis, ammonia and urinary catheter encrustation [3,5]. It is also a major cause of pathologies induced by *Helicobacter pylori* (HP) as this allows bacteria to survive at the low pH of the stomach and hence plays an important role in producing peptic and gastric ulcers [3]. As a result, ureases have been identified as important targets in research both for human and animal health, as well as in agriculture. For example, urease inhibitors have potential as antiulcer drugs [6]. Strategies based on urease inhibition are the first treatment of infections caused by urease producing bacteria. In agriculture, high urease activity releases abnormally large amounts of ammonia into the atmosphere after urea application and causes significant environmental problems and economical loss.

At present, crystallographic structures are available for only a few of the bacterial ureases [7–10]. However, the highly conserved amino acid sequences of all known ureases and the constant presence of two Ni ions, which are bridged by the carboxylate group of the carbamylated lysine and coordinated by surrounding histidine and aspartic residues, suggests a common catalytic pathway [5,8,9].

Canavalia ensiformis urease, Jack bean urease (JBU) consists of six subunits, each made of 840 residues, whereas *Klebsiella aerogenes* urease (KAU) has three subunits (α, β and γ) with 101, 106, and 506 residues, respectively [11]. The αβγ fragments of KAU are highly homologous to the single subunit of JBU. The structure of Bacillus pasteurii urease (BPU) reveals an analogous αβγ quaternary structure and a similar active site geometry [12].

Computer-assisted techniques have emerged as important tools in the search for new leads [13]. In the present study, we applied a combined ligand- and target-based drug design approach, which finally enabled us to identify a novel class (2-aminothiophenes) of urease inhibitors. Two of these inhibitors were found to be more active than the standard, acetohydroxamic acid.

2. Materials and methods

2.1. Pharmacophore generation

Pharmacophore modeling was performed by GASP, implemented in SYBYL 6.9 [14], using default parameters. GASP employs a genetic algorithm for the determination of relationships between functional groups in the superimposed ligands and the alignment

* Corresponding authors. Tel.: +92 21 4824910; fax: +92 21 4819018/19.
E-mail addresses: hassaan2@super.net.pk (K.M. Khan), zaheer.qasmi@iccs.edu (Z. Ul-Haq).
[1] Both authors contributed equally to the manuscript.

1093-3263/$ – see front matter © 2010 Elsevier Inc. All rights reserved.
doi:10.1016/j.jmgm.2010.02.004

of these groups in a common geometry for receptor binding. All aromatic rings and hydrogen binding (HB) sites are automatically recognized as potential pharmacophores.

Prior to the GASP run, the protonation states of the compounds were set according to physiological pH. Molecules with no ionizable moieties were taken as neutral. Then all structures were assigned the Gasteiger Marselli charges and minimized by using the Tripos force field method (Powell method, 0.05 $kcal^{-1}$ Å convergence criteria).

2.2. Virtual screening

The derived model was used to perform a pharmacophore-based search in a 3D database to identify 'hits' that satisfy the chemical and geometrical requirements using UNITY module of SYBYL 7.3. UNITY's conformationally flexible 3D searching was executed on an *in-house* library consisting of over 3,000 compounds. Lipinski's "Rule of five" was used to describe the drug-like properties. Drug likeness is a property that is most often used to characterize novel lead compounds [15] by screening of structural libraries. According to this rule, poor absorption is expected if MW > 500, log $P > 5$, hydrogen bond donors > 5, and hydrogen bond acceptors > 10 [16].

2.3. Molecular docking

Docking studies were performed using GOLD 4.0 (the Cambridge Crystallographic Data Center, UK) [17]. GOLD uses a genetic algorithm for docking flexible ligands into protein binding sites. It is therefore used to explore the full range of ligand conformational flexibility with partial protein flexibility [18]. The active site is defined as atoms of the protein within 10 Å of any ligand atom in the experimental protein–ligand complex (PDB entry code 4UBP). During this study, 10 docking solutions were generated for each structure, with early termination of the process if the respective RMSDs of the three highest ranked docking solutions were within 1.5 Å of each other. The default software settings were used for controlling of the parameters of GOLD's genetic algorithm. Since GOLD is not completely parameterized for nickel ions, the nickel atoms of urease were replaced by zinc during this study. This choice was based on an earlier observation of Shukla et al. [19,20] who reported that such a replacement of metal atoms during molecular docking has little or no effect on the structure of protein. Before the docking run all the water molecules from the protein structure were removed and hydrogen atoms were added.

3. Biological protocols

3.1. Urease inhibition assay

To perform urease inhibition with *Canavalia ensiformis* urease (U-1500) and *Bacillus pasteurii* urease (U-7127), two reaction mixtures, comprising 25 μL of each enzyme and 55 μL of buffers containing 100 mM urea, were incubated with 5 μL of test compounds (1 mM concentration) at 30 °C for 15 min in 96-well plates. Urease activities were determined by measuring the release of ammonia by using the indophenol method, as described by Weatherburn [21]. Briefly, 45 μL each of phenol reagents (1%, w/v phenol and 0.005%, w/v sodium nitroprusside) and 70 μL of alkali reagent (0.5%, w/v NaOH and 0.1% active chloride NaOCl) were added to each well. The absorbance at 630 nm was measured after 50 min, using a microplate reader (SpectraMax, Molecular Devices, CA, USA). All reactions were performed in triplicate in a final volume of 200 μL. The results (change in absorbance per min) were processed using SoftMax Pro software (Molecular Devices, CA, USA). All the assays were performed at pH 8.2 (0.01 M $K_2HPO_4{\cdot}3H_2O$, 1 mM EDTA and 0.01 M $LiCl_2$). Percentage inhibitions were calculated from the formula $100 - (OD_{testwell}/OD_{control}) \times 100$. Acetohydroxamic acid was used as the standard inhibitor of urease.

3.2. Phytotoxicity evaluation assay

This test was performed according to the modified protocol of McLaughlin et al. [22]. The test compounds were incorporated with sterilized E-medium at different concentration [23], *i.e.* 1000, 100 and 10 μg/ml in methanol. Sterilized conical flasks were inoculated with compounds of desired concentrations, prepared from the stock solution, and allowed to evaporate overnight. Each flask was inoculated with 20 mL of sterilized E-medium and ten *Lemna aequinocitalis* Welv. plants, each containing a rosette of three fronds. Other flasks were supplemented with methanol serving as negative control while phosphoroamide was used as positive control (Table 2).

Treatments were replicated three times and the flasks were incubated at 30 °C in a Fisons Fi-Totron 600 H Growth cabinet for 7 days, 9000 lx light intensity, 56 ± 10 rh (relative humidity), and 12 h day length. Growth of *L. aequinocitalis* in test compound containing flask was determined by counting the number of fronds per dose and growth inhibition was calculated with reference to the negative control.

4. Results and discussion

4.1. Pharmacophore generation

A pharmacophore model defines a special arrangement of chemical features that are shared by different ligands and are obviously responsible for binding and, as a consequence, for biological activity of various compounds [24]. Such a model can be used as a tool in 3D database mining; thereby enhancing the number of active compounds in a virtual sense. Molecules for pharmacophore generation were selected on the basis of following criteria. First, each molecule should represent a specific class of urease inhibitors; second the molecule should have potent urease inhibitory activity; third it should have some functional groups, which could be used in pharmacophore search. Since GASP can effectively develop pharmacophore models only for a limited number of molecules [25,26], a small data set of three highly active and structurally diverse urease inhibitors (Fig. 1) were taken from the literature [27–29] to develop the pharmacophore model [30]. The pharmacophore was automatically developed by GASP without specifying any base molecule. However, GASP selects a base molecule itself and fit the remaining molecules on it to generate a pharmacophore model.

The pharmacophore model generated by GASP consists of positions and tolerances for two accepter atoms (AA1 and AA2), one donor atom (DA1) and one hydrophobic center (HYP1), as shown in Fig. 2.

4.2. Virtual screening

The derived pharmacophore model was used to search the 3D structures (SYBYL mol2 format) of an *in-house* database to identify 'hits' using the fast flexible option in UNITY module of SYBYL 7.3 [14]. Our *in-house* database of organic compounds consists of over 3,000 compounds, of which the 1,846 that conform to the modified Lipinski's Rule of five [31] were used for screening. Virtual screening identified 366 hits that fulfill the specified requirements of pharmacophore model for urease inhibition. These hits were submitted to docking analysis for further evaluation.

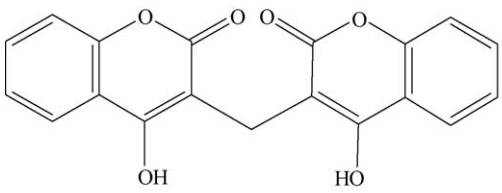

Biscoumarin Analog

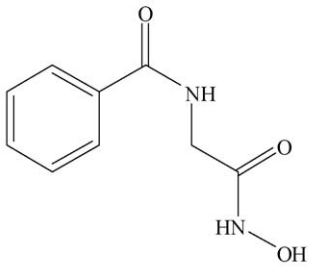

Hydroxamic Acid Analog

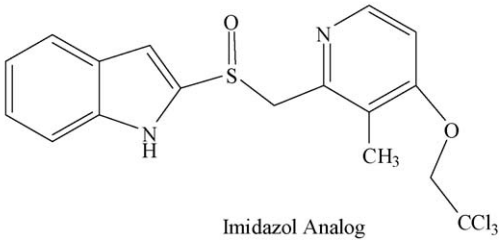

Imidazol Analog

Fig. 1. Structures of urease inhibitors used for pharmacophore model development.

4.3. Docking

Docking simulation was performed with *Bacillus pasteurii* urease (PDB Code: 4UBP) [32] using the genetic algorithm (GA) program GOLD. The key characteristic of a good docking program is its ability to reproduce the experimental binding modes of ligands and so on the reliability of the applied docking protocol was assessed by re-docking of the experimental complex to the binding site of *Bacillus pasteurii* urease as [33]. To test this, a ligand was taken out of the 3D structure of its protein–ligand complex. The docked binding mode was then compared with experimental binding mode, and an rmsd between the two was calculated; a prediction of binding mode was considered successful if the rmsd was below a certain value (usually 2.0 Å) [34]. The rmsd between the docked binding mode and the binding mode for acetohydroxamic acid in the crystallographic structure of BP urease was within this cut-off limit (0.60 Å). This protocol was then similarly applied for the docking of all ligands.

The binding modes for the 366 compounds identified by virtual screening were ranked according to the scoring function of GOLD. Initially the top ranked (high fitness scores) 100 compounds were selected from total of 366 compounds for further evaluation. After visual inspection, on the basis of binding modes (coordination to metal ions and hydrogen bonding to important active site residues) and structural diversity the most favorable compounds were selected. Furthermore, limited quantities and synthetic accessibility restricted us to select only top most compounds for the *in vitro* mechanism based assay. Based on the knowledge of existing urease inhibitors and the active site requirements together with the high scoring values of GOLD, we selected 13 compounds from the 100 highest scoring structures for *in vitro* biological testing. The synthesis of compounds **1**–**11** has been reported elsewhere [35,36], while compounds **12** and **13** were purchased from ACROS ORGANICS, Janssen pharmaceutical, Belgium, catalogue numbers 149231000 and 199250050, respectively. The structures of all 13 compounds are presented in Table 1.

4.4. Urease inhibition studies (in vitro)

Among the compounds screened, 2-aminothiophenes (**1**–**11**) were identified as active against the ureases of *Canavalia ensiformis* and *Bacillus pasteuri*, whereas compounds **12** and **13** showed no activity (Table 1). In the active compounds, the carbonyl oxygen, the nitrogen atom and the thiophene ring, respectively, matched with the HB acceptor, HB donor and hydrophobic features of the pharmacophore model (Fig. 3). Compound **5**, having a methyl group at C-4, was found to be the most potent among the series with IC_{50} = 2.81 and 0.83 μM against the two enzymes (*Canavalia ensiformis* and *Bacillus pasteuri*, respectively). Compounds **5** was also found to be more active than the standard inhibitor, with an IC_{50} value of 24.1 ± 0.71 and 22.21 ± 0.23 μM, respectively, for both

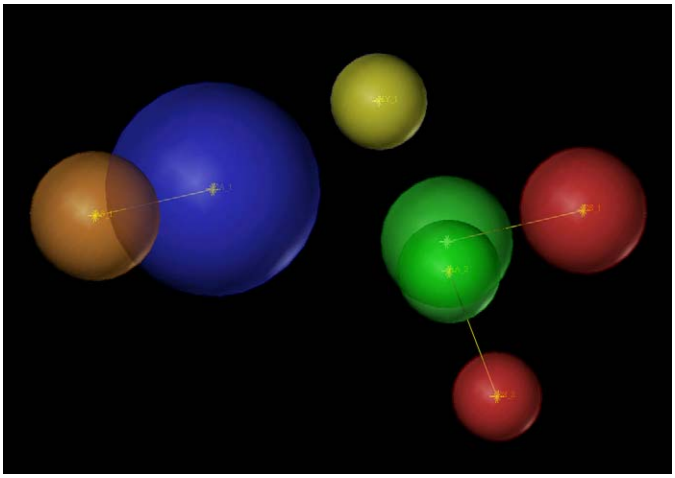

Fig. 2. Pharmacophore model generated by GASP for urease inhibitors containing two acceptor atoms (green sphere), one donor atom (blue sphere), two donor sites (red sphere), one acceptor site (orange sphere) and one hydrophobic centre (yellow sphere). The sphere size represents query tolerance.

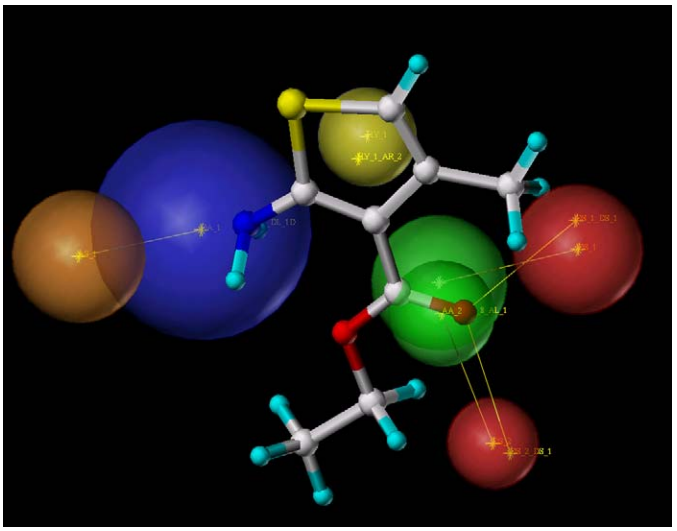

Fig. 3. Pharmacophore mapping of the most active compound **5** on the model developed by GASP.

Table 1
Inhibition of urease by compounds **1**–**13**.

Compound	Structure	$IC_{50} \pm$ S.E.M.[a] in μM	
		Canavalia ensiformis	*Bacillus pasteuri*
1	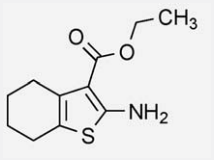	9.30 ± 0.0030	5.34 ± 0.0010
2	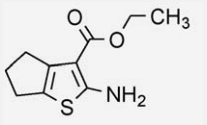	5.04 ± 0.0043	2.13 ± 0.0002
3	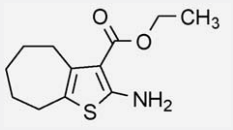	16.58 ± 0.0020	11.07 ± 0.0011
4	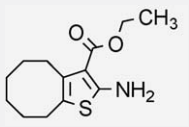	31.84 ± 0.0053	28.01 ± 0.0031
5	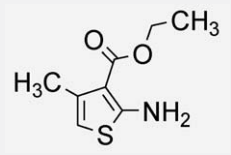	2.81 ± 0.0018	0.83 ± 0.0021
6	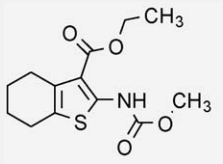	18.32 ± 0.0025	24.95 ± 0.0004
7	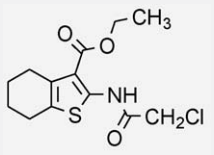	12.42 ± 0.0035	6.35 ± 0.0031
8	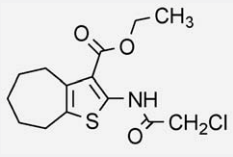	29.08 ± 0.0017	27.11 ± 0.0008
9	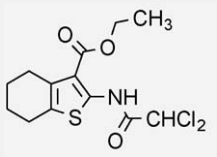	19.45 ± 0.0021	13.21 ± 0.0007

Table 1 (*Continued*)

Compound	Structure	$IC_{50} \pm$ S.E.M.[a] in μM	
		Canavalia ensiformis	*Bacillus pasteuri*
10	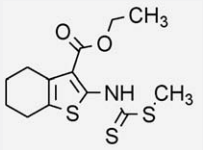	10.54 ± 0.0026	13.69 ± 0.0031
11	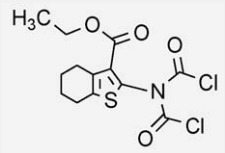	2.99 ± 0.0013	0.77 ± 0.0064
12	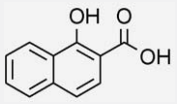	Not active	Not active
13	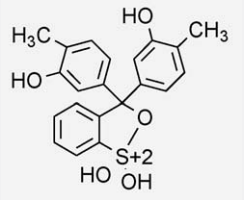	Not active	Not active
	Acetohydroxamic acid[b]	24.1 ± 0.71	22.21 ± 0.23

[a] S.E.M. is the standard error of the mean.
[b] Acetohydroxamic acid = std. inhibitor.

types of ureases. Compound **1** with a fused-cyclohexane ring showed IC_{50} = 9.30 and 5.34 μM and compound **2** with a fused-cyclopentane ring was found to have IC_{50} = 5.04 and 2.13 μM for the two ureases, respectively. Compound **3** with a fused-cycloheptane ring exhibited an IC_{50} = 16.58 and IC_{50} = 11.07 μM and compound **4** with a fused-cyclooctane ring showed IC_{50} = 31.84 and 28.01 μM for the two ureases, respectively. It is obvious that an increase in size of substituents from methyl to bulky fused cyclopentane, cyclohexane, cycloheptane and cyclooctane rings decreases the activity. The docking study showed that the fused bulky rings keep the metal coordinating thiophene ring at a distance from the nickel ions and thus decrease the coordinating tendency of these compounds. That might be one of the reasons which make these compounds, *i.e.* **3** and **4**, less active compared to compound **5** in which the thiophene ring is closer to the bimetallic nickel center (Fig. 4).

The activity also decreases when chloroacetyl, dichloroacetyl, thioester and methoxy carbonyl groups are attached to the amino

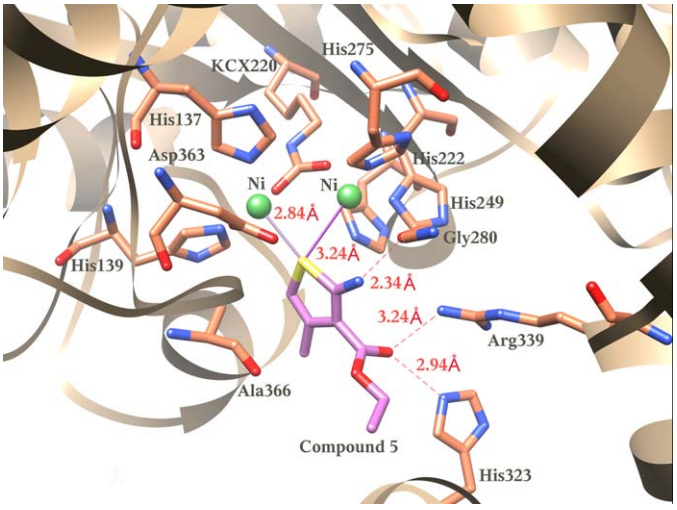

Fig. 4. Docking of compound **5** in the active site of BP urease. The purple line indicated coordination between nickel ions and ligand atoms whereas the red dotted line represented hydrogen bonding between ligand atoms and active site residues.

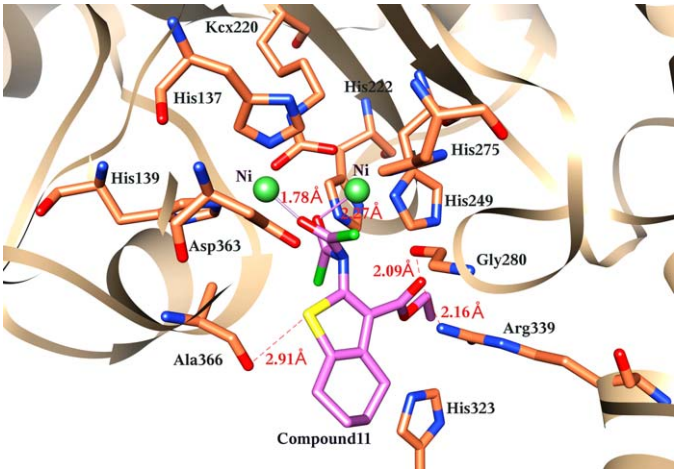

Fig. 5. Compound **11** docked into the binding site of BP urease. The purple line indicated coordination between nickel ions and ligand atoms whereas the red dotted line represented hydrogen bonding between ligand atoms and active site residues.

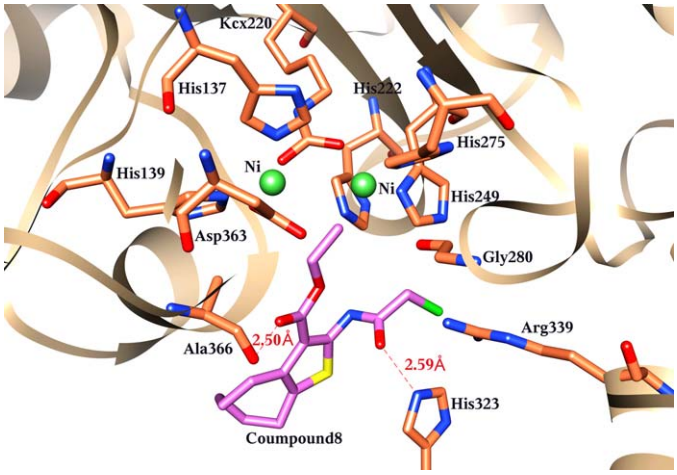

Fig. 6. Docked conformation of compound **8** in the active site of BP urease. The red dotted line represented hydrogen bonding between ligand atoms and active site residues.

group of the parent compound, as in case of compound **7** having chloroacetyl group (IC_{50} = 12.42 and 6.35 μM for the both ureases, respectively). Compound **8** with a bulky cycloheptyl group, in addition to the chloroacetyl group, possessed IC_{50} = 29.08 and 27.11 μM for the two ureases, respectively, while compound **9,** with a dichloroacetyl group, showed IC_{50} = 19.45 μM for *Canavalia ensiformis* and IC_{50} = 13.21 μM for *Bacillus pasteuri*. Compound **10** with a thiocarbamate group has an IC_{50} of 10.54 and 13.69 μM for the two ureases, respectively, while **6,** with a methyl ester group, has an IC_{50} of 18.32 and 24.95 μM for *Canavalia ensiformis* and *Bacillus pasteuri*, respectively. Compound **11** with a dicarbomimidicdichloride group was also found to be potent with IC_{50} of 2.99 and 0.77 μM for *Canavalia ensiformis* and *Bacillus pasteuri*, respectively (Table 1). From the structure of the docking confirmation it appears that the greater activity of compound **11** might be due to the two carbonyl oxygens which are in close proximity of two nickel atoms and may therefore form a stable complex (Fig. 5). It was also observed that compounds having substitutions on the amino group generally showed less activity as compare to compounds having no substituents on this position. The substituent on amino group might keep the thiophene ring at a distance from the nickel center, thus lowering the activity (Fig. 6).

As urease inhibitors are used in agriculture practices for the prevention of soil urea deterioration, a phytotoxicity profile of this new class of inhibitors was also assessed. The results of assay showed that compounds **1**–**11** are non-toxic to the plants (Table 2).

Table 2
Results of *Lemna aequinocitalis* Welv. phytotoxicity bioassay.

Compound	Conc. of compound (μg/mL)		
	1000	100	10
1	75.00	00.00	−12.5
2	100	42.06	15.09
3	100	100	100
4	100	100	41.66
5	89.5	25.00	9.00
6	100	62.50	16.60
7	100	54.20	17.50
8	67.3	32.99	13.00
9	100	50.00	41.66
10	100	41.00	13.00
11	80.6	39.00	16.03
Phosphoroamide	100	60.3	35.0

4.5. Comparison of the pharmacophore model with the binding site of BP urease

The features in the derived pharmacophore model were compared with the structure of compound **5** as it docks into the binding site of BP urease (Figs. 3 and 4).

A marked similarity was observed between the pharmacophore and the ligand binding features in the docked structure. The docking study suggests that the carbonyl oxygen of compound **5** is hydrogen-bonded to the amino group of Arg 339, and indol of His 323 of urease. This interaction corresponds to a hydrogen bond acceptor (HBA) feature in the pharmacophore model, mapping the same carbonyl oxygen as HBA, as well as two donor sites, Arg 339 and His 323, on the receptor.

The amino group of compound **5** showed hydrogen bond donor (HBD) feature in the pharmacophore model, which corresponds to proposed hydrogen bonding between the nitrogen of amino group in compound **5** and the oxygen of the carboxylate group in Gly 280. Finally, mapping of the thiophene ring of compound **5**, based on hydrophobic features in pharmacophore model, suggested the existence of corresponding hydrophobic feature in the active site.

5. Conclusion

In this study, we conducted a virtual screening of an *in-house* library of over 3,000 compounds to identify effective urease inhibitors. We employed ligand-based pharmacophore modeling for *in silico* screening. Molecular docking was employed for further screening of the 'hit' compounds. By this approach, a novel class for the urease inhibitors was successfully identified. Substituted 2-aminothiophenes and their derivatives **1**–**11** have the potential to inhibit urease. Structure–activity relationship shows that bulky substituents cause a loss in activity apparently due to the torsional strain. Furthermore, it was concluded that substitution at the amino group of compound **1** also cause changes in the activity profile.

Two compounds, *i.e.* compound **5** and **11**, in this class showed remarkable urease inhibitory activity. The experimental validation of our pharmacophore model will contribute in lead optimization by chemical derivatization of active compounds, identified during the current study.

Acknowledgements

We acknowledge the Higher Education Commission (HEC) Pakistan for financial assistance under "National Research Program for Universities". We gratefully acknowledge the valuable technical support by Prof. Bernd Michael Rode and Prof. John McGrady for proofreading the manuscript.

References

[1] N.E. Dixon, T.C. Gazzola, R.L. Blakeley, B. Zermer, Letter: Jack bean urease (EC 3.5.1.5). A metalloenzyme. A simple biological role for nickel? J. Am. Chem. Soc. 97 (1975) 4131–4133.
[2] J.B. Sumner, The isolation and crystallization of the enzyme urease: preliminary to paper, J. Saw Chem. 69 (1926) 435–441.
[3] H.L.T. Mobley, R.P. Hausinger, Microbial ureases: significance, regulation, and molecular characterization, Microbiol. Rev. 53 (1989) 85–108.
[4] B. Krajewska, Ureases: roles, properties and catalysis, Wiad. Chem. 56 (2002) 223–253.
[5] H.L.T. Mobley, M.D. Island, R.P. Hausinger, Molecular biology of microbial ureases, Microbiol. Rev. 59 (1995) 451–480.
[6] (a) Y. Onoda, T. Magaribuchi, H. Tamaki, Effects of the new anti-ulcer agent 12-sulfodehydroabietic acid monosodium salt on duodenal alkaline secretion in rats, Arzneimittelforschung 40 (1990) 576–578;
(b) Y. Onoda, M. Takido, T. Magaribuchi, H. Iwasaki, Effects of 12-sulfodehydroabietic acid monosodium salt (TA-2711), a new anti-ulcer agent, on gastric mucosal lesions induced by necrotizing agents and gastric mucosal defensive factors in rats, Jpn. J. Pharmacol. 52 (1990) 631–638.

[7] A. Bairoch, R. Apweiler, The SWISS-PROT protein sequence database and its supplement TrEMBL in 2000, Nucleic Acids Res. 28 (2000) 45–48.
[8] A. Bateman, E. Birney, L. Cerruti, R. Durbin, L. Etwiller, S.R. Eddy, S. Griffiths-Jones, K.L. Howe, M. Marshall, E.L.L. Sonnhammer, The Pfam protein families database, Nucleic Acids Res. 30 (2002) 276–278.
[9] H.M. Berman, J. Westbrook, Z. Feng, G. Gilliland, T.N. Bhat, H. Weissig, I.N. Shindyalov, P.E. Bourne, The protein data bank, Nucleic Acids Res. 28 (2000) 235–242.
[10] S. Benini, W.R. Rypniewski, K.S. Wilson, S. Miletti, S. Ciurli, S. Mangani, A new proposal for urease mechanism based on the crystal structures of the native and inhibited enzyme from Bacillus pasteurii: why urea hydrolysis costs two nickels, Structure 7 (1999) 205–216.
[11] S. Benini, W.R. Rypniewski, K.S. Wilson, S. Ciurli, S. Mangani, Structure-based rationalization of urease inhibition by phosphate: novel insights into the enzyme mechanism, J. Biol. Inorg. Chem. 6 (2001) 778–790.
[12] S. Ciurli, S. Benini, W.R. Rypniewski, K.S. Wilson, S. Miletti, S. Mangani, Structural properties of the nickel ions in urease: novel insights into the catalytic and inhibition mechanisms, Coord. Chem. Rev. 190 (1999) 331–355.
[13] G.K. Farber, New approaches to rational drug design, Pharmacol. Ther. 84 (1999) 327–332.
[14] SYBYL 6.9, Tripos, Inc., 1699 South Hanley Road, St. Louis, MO 63144, 2006.
[15] I. Muiegge, Selection criteria for drug-like compounds, Med. Res. Rev. 23 (2003) 302–321.
[16] C.A. Lipinski, F. Lombardo, B.W. Dominy, P.J. Feeney, Experimental and computational approaches to estimate solubility and permeability in drug discovery and development settings, Adv. Drug Deliv. Rev. 23 (1997) 3–25.
[17] G. Jones, P. Willett, R.C. Glen, A.R. Leach, R. Taylor, Development and validation of a genetic algorithm for flexible docking, J. Mol. Biol. 267 (1997) 727–738.
[18] Gold Version 1.2 ed., Astex Technology, Cambridge, UK, 2001.
[19] K.L. Shukla, T.M. Gund, S.R. Meshnick, Molecular modeling studies of the artemisinin (qinghaosu)–hemin interaction: docking between the antimalarial agent and its putative receptor, J. Mol. Graph. 13 (1995) 215–222.
[20] C. Feng, S. Jianhua, L. Xiaomin, Z. Weiliang, G. Jiande, J. Ruyun, J. Hualiang, C. Kaixian, Molecular docking and 3-D-QSAR studies on the possible antimalarial mechanism of artemisinin analogues, Bioorg. Med. Chem. 10 (2002) 2883–2891.
[21] M.W. Weatherburn, Phenol–hypochlorite reaction for determination of ammonia, Anal. Chem. 39 (1967) 971–974.
[22] (a) J.L. McLaughlin, C.-J. Chang, D.L. Smith, Studies in natural products chemistry, "bench-top" bioassays for the discovery of bioactive natural products: an update, in: Atta-ur-Rahman (Ed.), Structure and Chemistry (Part-B), vol. 9, Elsevier Science Publishers B.V., The Netherlands, 1991, p. 383;
(b) B.N. Meyer, N.R. Ferrigni, J.E. Putnam, L.B. Jacobsen, D.E. Nichols, J.L. McLaughlin, Brine shrimp: a convenient general bioassay for active plants constituents, Planta Med. 45 (1982) 31–34;
(c) D.J. Finney, Probit Analysis, 3rd ed., Cambridge University Press, Cambridge, 1971.
[23] J.A. Finkelstein, R.M. Kenan, J. Weinstock, Eur. Patent 403,159, December 19 (1990) (to Smithkline Beecham Corp.).
[24] H.J. Bom, G. Klebe, H. Kubinyi, Wirksotffdesign (Active Substance Design), Spektrum Akademischer Verlag Gumb H, Heildelberg/Berlin/Oxford, 1996.
[25] H. Yuan, A.P. Kozikowski, P.A. Petukhov, CoMFA study of piperidine analogues of cocaine at the dopamine transporter: exploring the binding mode of the 3α-substituent of the piperidine ring using pharmacophore-based flexible alignment, J. Med. Chem. 47 (2004) 6137–6143.
[26] I.J. Mcfadyen, H. Houshyar, L.Y. Liu-Chen, J.H. Woods, J.R. Traynor, The steroid 17α-acetoxy-6-dimethylaminomethyl-21-fluoro-3-ethoxy-pregna-3,5-dien-20-one (SC17599) is a selective μ-opioid agonist: implications for the μ-opioid pharmacophore, Mol. Pharmacol. 58 (2000) 669–676.
[27] T.C. Kuhler, J. Fryklund, N.A. Bergman, J. Weilitz, A. Lee, H. Larsson, Structure–activity relationship of omeprazole and analogues as *Helicobacter pylori* urease inhibitors, J. Med. Chem. 38 (1995) 4906–4916.
[28] M. Satoh, K. Munakata, K. Kitoh, N. Seto, T. Kanazawa, H. Takeuchi, O. Yoshida, Therapy for urolithiasis with hydroxamic acids. IV. Prevention of infected urinary stone formation with N-(pivaloyl)glycinohydroxamic acid, J. Pharmacobiodyn. 4 (1981) 469–474.
[29] K.M. Khan, S. Iqbal, M.A. Lodhi, G.M. Maharvi, Z. Ullah, M.I. Choudhary, A.U. Rahman, S. Perveen, Biscoumarin: new class of urease inhibitors; economical synthesis and activity, Bioorg. Med. Chem. 12 (2004) 1963–1968.
[30] G. Jones, P. Willett, R.C. Glen, A genetic algorithm for flexible molecular overlay and pharmacophore elucidation, J. Comput. Aided Mol. Des. 9 (1995) 532–549.
[31] C.A. Lipinski, F. Lombardo, B.W. Dominy, P.J. Feeney, Experimental and computational approaches to estimate solubility and permeability in drug discovery and development settings, Adv. Drug Deliv. Rev. 46 (2001) 3–26.
[32] S. Benini, W.R. Rypniewski, K.S. Wilson, S. Miletti, S. Ciurli, S. Mangani, The complex of Bacillus pasteurii urease with acetohydroxamate anion from X-ray data at 1.55 Å resolution, J. Biol. Inorg. Chem. 5 (2000) 110–118.
[33] G. Folkers, in: P.W. Codding (Ed.), Structure-based Drug Design Experimental and Computational Approaches, Kluwer Academic Publishers, Norwell, MA, 1998, p. 271.
[34] N. Singh, G.L. Cheve, D.M. Ferguson, C.R. McCurdy, A combined ligand-based and target-based drug design approach for G-protein coupled receptors: application to salvinorin A, a selective kappa opioid receptor agonist, J. Comput. Aided Mol. Des. 20 (2006) 471–493.
[35] N.P. Peet, S. Sunder, R.J. Barbuch, A.P. Vinogradoff, Mechanistic observations in the Gewald syntheses of 2-aminothiophenes, J. Heterocycl. Chem. 23 (1986) 129–134.
[36] K.M. Khan, Zia-Ullah, M.A. Lodhi, J. Saima, M.I. Choudhary, Atta-ur-Rahman, Synthesis and anti-inflammatory activity of some selected aminothiophene analogs, J. Enz. Inhibit. Med. Chem. 21 (2006) 139–143.